Spectrochimica Acta Part A 79 (2011) 39–44

Contents lists available at ScienceDirect

Spectrochimica Acta Part A: Molecular and Biomolecular Spectroscopy

journal homepage: www.elsevier.com/locate/saa

Synthesis, spectral characterization and biological activities of Mn(II) and Co(II) complexes with benzyloxybenzaldehyde-4-phenyl-3-thiosemicarbazone

B. Prathima [a], Y. Subba Rao [a], G.N. Ramesh [a], M. Jagadeesh [a], Y.P. Reddy [b], P.V. Chalapathi [a], A. Varada Reddy [a,*]

[a] Analytical Division, Department of Chemistry, Srivenkateswara University, Tirupati 517502, India
[b] Department of Physics, Sri Padhmavati Mahila Visva Vidyalayam (Women's University), Tirupati 517502, India

ARTICLE INFO

Article history:
Received 8 November 2010
Received in revised form 8 January 2011
Accepted 17 January 2011

Keywords:
Thiosemicarbazone
Electronic spectra
EPR spectra
X-ray powder diffraction

ABSTRACT

Mn(II) and Co(II) complexes of benzyloxybenzaldehyde-4-phenyl-3-thiosemicarbazone have been synthesized and characterized by the investigations of electronic and EPR spectra and X-ray diffraction. Based on the spectral studies, an octahedral geometry is assigned for the Mn(II) and Co(II) complexes. X-ray powder diffraction studies reveal that Mn(II) and Co(II) complexes have triclinic crystal lattices. The unit cell parameters of the Mn(II) complex are $a = 11.0469$ Å, $b = 6.2096$ Å, $c = 7.4145$ Å, $\alpha = 90.646^\circ$, $\beta = 95.127^\circ$, $\gamma = 104.776^\circ$, $V = 489.7$ Å^3 and those of Co(II) complex are $a = 9.3236$ Å, $b = 10.2410$ Å, $c = 7.8326$ Å, $\alpha = 90.694^\circ$, $\beta = 99.694^\circ$, $\gamma = 100.476^\circ$, $V = 724.2$ Å^3. When the free ligand and its metal complexes are subjected to antibacterial activity, the metal complexes are proved to be more active than the ligand. However with regard to in vitro antioxidant activity, the ligand exhibits greater antioxidant activity than its metal(II) complexes.

1. Intoduction

Thiosemicarbazones usually act as chelating ligands with transition metal ions, bonding through the sulphur and hydrazine nitrogen atoms. Thiosemicarbazones and their complexes have received considerable attention because of their pharmacological activities [1]. The metal complexes show more pharmacological activities as compared to the free thiosemicarbazones and semicarbazones [2]. The thiosemicarbazones have numerous applications like antitumour [3], fungicides and antibacterial [4], antiviral [5], antifungal [6], anti HIV [7], anticancer [8] and other biological activities [9]. Particularly the thiosemicarbazones can be used as reagents for Co(II), Ni(II), Cu(II) and Pd(II) for high performance liquid chromatography and diverse biological activities [10–13]. Thiosemicarbazones have also been used as analytical reagents for the analysis of metals [14] and as devices for optical storage and optical information processing [15]. Novak et al. have reported that salicylaldehyde-4-phenylthiosemicarbazone belongs to an important class of biologically active thiosemicarbazone compounds that possess anticancer, antivirial, antibacterial, antiinflammatory and antifungal activity [16].

2. Experimental methods

2.1. Materials

All the chemicals used are of analytical grade. Organic chemicals such as thiobarbituric acid (TBA), trichloroaceticacid (TCA), α-tocopherol, butylated hydroxy toluene (BHT), 1,1-diphenyl-2-picryl hydrazyl (DPPH), 4-phenyl thiosemicarbazide and dimethyl formamide (DMF) are procured from Sigma–Aldrich and all metal salts are procured from E. Merck Chemical Company.

2.2. Physical measurements

The IR spectra of the compounds are recorded on a Nikolet FT-IR 560 Magna spectrometer using KBr (neat). The Bruker 300 MHz NMR spectrometer is used to obtain the ^{1}H NMR spectrum of the ligand. A mass spectrum is recorded in a Quattro LC-Micro mass. Elemental analysis is obtained from vario-micro qub elementar analyzer. The electronic spectra of the complexes are recorded on a Perkin Elmer UV-Visible Lambda 950. EPR spectra are recorded on an EPR spectrometer (JEOL FE-1X), operating in the X-band frequencies with a modulation frequency of 100 kHz. For EPR measurements, 100 mg of each compound is taken in a quartz tube. The magnetic field is scanned from 2200 to 4200 G, with a scan speed of 250 G min^{-1}. Absorbance is measured using Systronics UV/VIS spectrometer-117. A digital pH meter (model L1-10 Elico, India) is used for measuring pH. X-ray diffractometer (PHILIPSPW3710)

* Corresponding author. Tel.: +91 877 2249666x303; fax: +91 877 2249611.
E-mail address: ammireddyv@yahoo.co.in (A. Varada Reddy).

1386-1425/$ – see front matter © 2011 Elsevier B.V. All rights reserved.
doi:10.1016/j.saa.2011.01.029

using CuK_α (1.5418 Å) radiation operated at 45 kV and 25 mA is used in X-ray investigations.

2.3. Synthesis of the ligand and their metal complexes

Equal volumes of hot ethanolic solution containing 2.12 g of benzyloxybenzaldehyde and hot ethanolic solution containing 1.67 g of 4-phenyl-3-thiosemicarbazide are mixed. The mixture obtained is refluxed for an hour, then stirred for 3½ h at 60–70 °C and kept at room temperature for a day. The resulting intense yellow colored precipitate is filtered, washed with ethanol and dried. The schematic structure is depicted below [17].

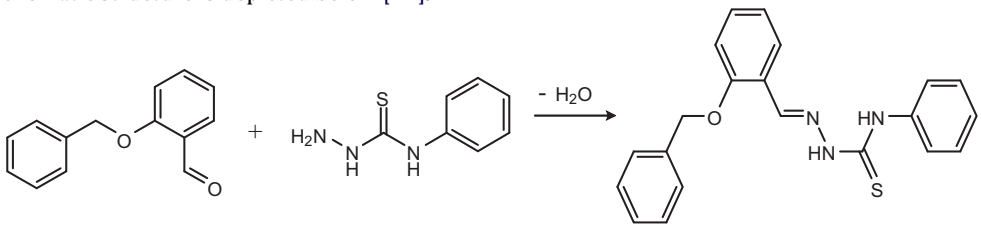

Benzyloxybenzaldehyde 4-Phenyl-3-thiosemicarbazide Benzyloxybenzaldehyde-4- phenyl-3-thiosemicarbazone

2.3.1. Synthesis of metal complexes

A mixture of hot ethanolic solution (10 ml) of free ligand (0.002 mol) and hot ethanolic solution (10 ml) of (0.001 mol) the metal solutions [$MnCl_2{\cdot}4H_2O/CoCl_2{\cdot}6H_2O$] was refluxed for 3–4 h and 6–7 h at 50–60 °C, respectively. The resulting solutions are allowed to stand at room temperature and upon slow evaporation gives cream colored crystals of Mn(II) complex and brick red colored crystals of Co(II)complex. The crystals are collected, washed with 50% ethanol and dried. The purity of the complex is checked by TLC.

2.4. Antibacterial screening

In vitro antibacterial screening is performed by the agar disc diffusion method [18,19]. The bacterial species used in the screening are gram-negative bacteria such as *Klebsiella pneumoniae* and *Escherichia coli* and gram-positive bacteria such as *Staphylococcus aureus* and *Bacillus subtilis*. Stock cultures of the test bacterial species are maintained on nutrient agar media (Hi-media laboratories, Mumbai) by subculturing in Petri dishes. The media are prepared by adding the components as per manufacturer's instructions and sterilized in the autoclave at 121 °C and atmospheric pressure for 15 min. Each medium is cooled to 45–60 °C and 20 ml of it is poured into a Petri dish and allowed to solidify. After solidification, Petri plates with media are spread with 1.0 ml of bacterial suspension prepared in sterile distilled water. The wells are bored with cork borer and the agar plugs are removed. To each agar well, 100 ml of the compound reconstituted in DMF of concentration 1.0 mg/ml is added. DMF is used as a negative control and in similar way, antibiotics such as ampicillin and tetracycline are used as positive control standards. All the plates are incubated at 37 °C for 24 h and they are observed for the growth inhibition zones. The presence of clear zones around the wells indicate that both the ligand and complexes are active. The diameter of zone of inhibition is calculated in millimeters. The well diameter is deducted from the zone diameter to get the actual zone of inhibition diameter and the values are tabulated.

2.5. DPPH scavenging activity

The principle for the reduction in DPPH free radicals is that the antioxidant reacts with stable free radical DPPH and converts it to 1,1-diphenyl-2-picrylhydrazine. The ability to scavenge the stable free radical DPPH is measured by decrease in the absorbance at 517 nm. Solutions ligand and its Mn(II) and Co(II) complexes at 100 μM concentrations are added to 100 μM DPPH and kept in ethanol tubes. The tubes are kept at ambient temperature for 20 min and absorbances are measured at 517 nm. For positive control, α-tocopherol is used [20]. These measurements are run in triplicate. The percentage of scavenging activity is calculated as follows:

$$\text{scavenging activity}\,(\%) = \frac{A_{\text{DPPH}} - A_{\text{TEST}}}{A_{\text{DPPH}}} \times 100 \quad (1)$$

where A_{DPPH} is the absorbance of DPPH without test sample (control) and A_{TEST} is the absorbance of DPPH in the presence of test sample.

2.6. Inhibition of lipid peroxidation in rat brain homogenate

2.6.1. Preparation of rat brain homogenate

For the present study, Albino Wistar rats (180–200 g) are selected. Prior to decapitation and removal of the brain, the animals are anesthetized with ether and perfused transcardially with ice-cold normal saline to prevent contamination of brain tissue with blood. The collected tissues are weighed and their homogenates 10% w/v are prepared in 0.15 M KCl and centrifuged at 800 rpm for 10 min. The supernatants are used immediately for the study [21].

2.6.2. Iron(III) induced lipid peroxidation

The incubation mixtures contain a final volume of 1.5 ml brain homogenate (0.5 ml of 10% (w/v)), KCl (0.15 M) and ethanol (10 μl) or test compound dissolved in ethanol. Peroxidation is initiated by adding ferric chloride (100 μM) to give the final concentration stated. After incubation for 20 min at 37 °C, reactions are stopped by adding 2 ml of ice-cold 0.25 M HCl containing 15% trichloroaceticacid (TCA), 0.38% thiobarbituric acid (TBA) and 0.05% butylated hydroxy toluene (BHT). The samples are heated at 80 °C for 15 min, cooled and centrifuged at 1000 rpm for 10 min. The absorbances of the supernatant solutions are measured at 532 nm. Percentage inhibition of thiobarbituricacid reactive substances (TBARS) formed by test compounds was calculated by comparing with the control. Iron(III) solutions are prepared afresh in distilled water and other solutions are prepared in 0.15 M KCl. Since most buffers trap hydroxyl radical or interfere with iron conversion, the reactions are carried out in unbuffered 0.15 M KCl solution [22,23].

The inhibition percentages of the selected ligand and its metal complexes are evaluated using lipid peroxidation method. The fol-

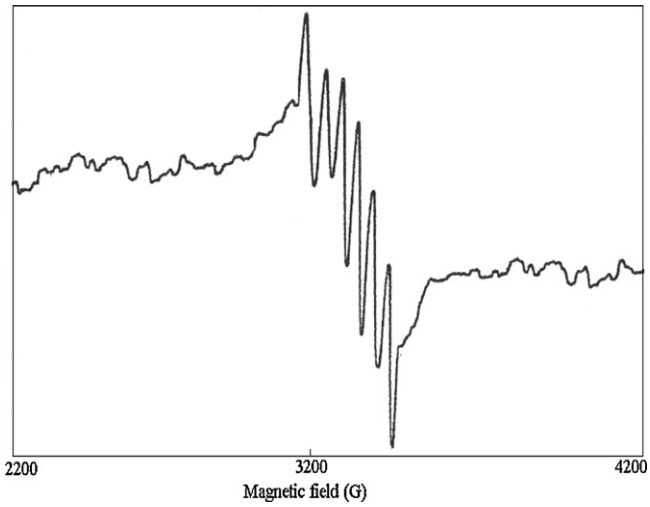

Fig. 1. Powder X-band EPR spectrum of Mn(II) at room temperature (ν = 9.205 GHz).

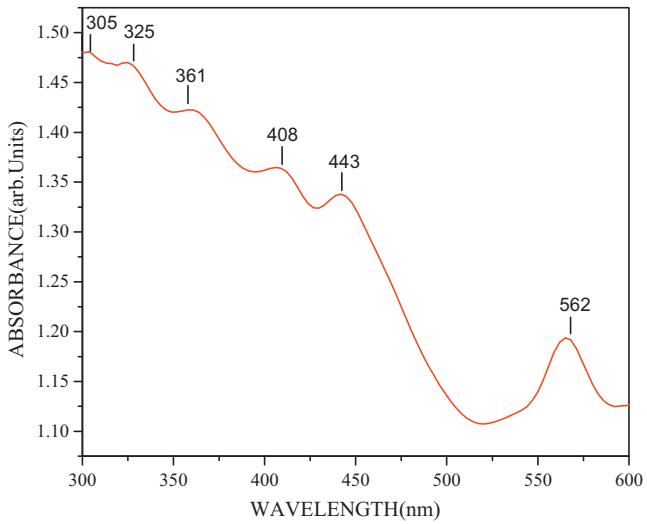

Fig. 2. Solid state electronic spectrum (nm) of Mn(II)complex.

lowing formula is used in calculating inhibition percentages:

$$\text{inhibition percentage} = \frac{A_{CONT} - A_{TEST}}{A_{CONT}} \times 100 \quad (2)$$

where A_{CONT} is the absorbance of the control reaction and A_{TEST} is the absorbance in the presence of the test sample.

3. Results and discussion

3.1. Characterization of the ligand

Benzyloxybenzaldehyde-4-phenyl-3-thiosemicarbazone is analyzed by IR and ^{1}H NMR spectroscopy. The IR spectrum of ligand exhibits absorption bands around 1543.18 cm^{-1} (C=N), 1253.18 cm^{-1}(C=S) and 3307.85 cm^{-1}(–NH). The ^{1}H NMR (300 MHz, δ (ppm), $CDCl_3$) investigations provide the following information 8.0–7.15 (m, 14H, Ar–H), 11.66 (s, NH), 5.13 (s, N=CH), 3.12 (s, OCH_2). Elemental analysis gives C 69.78; H 5.30; N 11.63; S 8.87; Calcd: C 69.32; H 5.043; N11.35; S 8.725%. The mass spectrum of ligand shows a molecular ion peak at 362.1, corresponding to the species $[C_{21}H_{19}N_3OS]^+$, which confirms the proposed formula. Benzyloxybenzaldehyde-4-phenyl-3-thiosemicarbazone is a yellow solid with a melting point of 150–152 °C.

3.2. Electron paramagnetic resonance spectrum of the Mn(II) complex

The EPR spectrum of Mn(II) complex is shown in (Fig. 1). EPR spectrum of Mn(II) exhibits sextet, superimposed on a broad line. The sextet slowly broadened leaving behind a single broad line due to dipole–dipole interaction. The EPR spectrum of Mn(II), in general, can be analyzed using the spin-Hamiltonian [24,25]:

$$H = g\beta B \cdot S + SAI + SDS$$

where g is the isotropic factor, β is the Bohr magneton, B is the external magnetic field, S is the vector operator of the electron spin momentum, A is the hyperfine interaction parameter, I is the vector operator of nuclear spin momentum and D is the zero field splitting parameter. Investigations of the EPR spectrum of Mn(II) complex have shown that it has been characterized by an intense resonance signal at around g = 2.0 with six line hyperfine pattern, which is a characteristic of ions with a nuclear spin, I = 5/2 [26].

The ability to observe the ^{55}Mn hyperfine structure has two tangible benefits: (i) it generally allows unambiguous assignments of positions of complex resonance lines to manganese and (ii) the magnitude of hyperfine splitting constant provides a measure of the bonding between Mn(II) ions and its surrounding ligands [27]. In case of d^5 transition metal ions, it is known that axial distortion of octahedral symmetry gives rise to three Kramer's doublets $|\pm5/2\rangle$, $|\pm3/2\rangle$ and $|\pm1/2\rangle$ [28]. Application of Zeeman field lifts the spin degeneracy of the Kramer's doublets [29]. As the crystal field splitting is normally much greater than the Zeeman field, the resonances observed are due to transitions within the Zeeman field split Kramer's doublets. The resonance at $g \sim 2.0$ is due to Mn(II) ions in an environment close to octahedral symmetry [30] and is known to arise from the transition between the energy levels of the lower doublet. The magnitude of hyperfine splitting constant (A) provides a measure of covalency between the Mn(II) ion and the ligand. The strength of the hyperfine splitting depends on the matrix into which the ion is dissolved and is mainly determined by the electro negativity of the neighbors. This means a qualitative measure of the covalency of the bonding in the matrix which can be determined from the value of A; the smaller the splitting, the more covalent the bonding of the anion. It is also noted that the g-value for the hyperfine splitting was indicative of the nature of bonding in the complex. If the g-value shows a negative shift with respect to 2.0023, then the bonding is ionic and conversely, if the shift is positive, then the bonding is more covalent in nature. In the present work, from the measured negative shift in the g-value, with respect to 2.0023, it is apparent that the Mn(II)ion is in an ionic environment. The g value calculated is 2.0183. The hyperfine coupling constant value is 102 G.

3.3. Electronic spectrum of the Mn(II) complex

The electronic spectrum of Mn(II) complex is shown in Fig. 2. The spectrum consists of six bands at 562, 443, 408, 361, 325 and 305 nm that are characteristics of Mn(II) in octahedral symmetry. The characteristic broad bands at longer wavelengths 562 and 443 nm are assigned, respectively to the low lying transitions $^6A_{1g}(S) \rightarrow {}^4T_{1g}(G)$ and $^6A_{1g}(S) \rightarrow {}^4T_{2g}(G)$. With the help of the Tanabe–Sugano diagram Other bands at 408, 361, 325 and 305 nm are assigned to the transitions $^6A_{1g}(S) \rightarrow {}^4A_1g(G) + {}^4Eg(G)$, $^6A_{1g}(S) \rightarrow {}^4T_{2g}(D)$, $^6A_{1g}(S) \rightarrow {}^4E_g(D)$ and $^6A_{1g}(S) \rightarrow {}^4T_{1g}(P)$, respectively [31]. The energy matrices for d^5 configuration with Trees correction (free ion term α = 76 cm^{-1}) are solved for various values of the crystal field parameter (Dq) and Racah parameters (B and C). The values Dq = 890, B = 870 and C = 3000 cm^{-1} give a reasonably

Table 1
Observed and calculated band positions of Mn(II) complex.

Transition	Observed band position		Calculated wave number (cm^{-1})
	Wave length (nm)	Wave numbers (cm^{-1})	
$^6A_{1g}(S) \rightarrow {}^4T_{1g}(G)$	562	17,789	17,816
$^6A_{1g}(S) \rightarrow {}^4T_{2g}(G)$	443	22,567	22,536
$^6A_{1g}(S) \rightarrow {}^4A_{1g}(G), {}^4E_g(G)$	408	24,503	25,207
$^6A_{1g}(S) \rightarrow {}^4T_{2g}(D)$	361	27,693	28,331
$^6A_{1g}(S) \rightarrow {}^4E_g(D)$	325	30,761	30,272
$^6A_{1g}(S) \rightarrow {}^4T_{1g}(P)$	305	32,777	32,815

good fit between observed and calculated values of the band head data Table 1.

3.4. Electron paramagnetic resonance spectrum of the Co(II) complex

EPR spectrum for Co(II)complex is not observed at normal lab temperature. This might be because of the broadening of the line due to rapid spin lattice relaxation of Co(II) at higher temperature [32]. Therefore EPR spectrum of Co(II) complex is recorded at liquid nitrogen temperature (LNT) and the calculated value of g is 2.1785.

3.5. Electronic spectrum of the Co(II) complex

The electronic spectrum of Co(II) complex exhibits three absorption bands at 1130, 600 and 520 nm. For Co(II) (d^7) in octahedral field without considering spin orbit interaction, three spin allowed transitions $^4T_{1g}(F) \rightarrow {}^4T_{2g}(F)$, $^4T_{1g}(F) \rightarrow {}^4A_{2g}(F)$ and $^4T_{1g}(F) \rightarrow {}^4T_{1g}(P)$ are to be expected. Of these transitions, $^4T_{1g}(F) \rightarrow {}^4A_{2g}(F)$ involves the promotion of two electrons and is expected to be weak [33]. Accordingly the two bands observed at 1130 nm (8847 cm^{-1}) and 520 nm (19226 cm^{-1}) are attributed to spin allowed transitions $^4T_{1g}(F) \rightarrow {}^4T_{2g}(F)$ and $^4T_{1g}(F) \rightarrow {}^4T_{1g}(P)$, where as the band observed at 600 nm (16662 cm^{-1}) is attributed to$^4T_{1g}(F) \rightarrow {}^4A_{2g}(F)$. In octahedral symmetry, theoretically, the ratio of the energies of the transitions $^4T_{1g}(F) \rightarrow {}^4A_{2g}(F)$ (ν_2) and $^4T_{1g}(F) \rightarrow {}^4T_{2g}(F)$ (ν_1) are almost invariable at 1.9–2.2 [34]. From the band positions Table 2, the ratio of ν_2/ν_1 is 1.9. The cubic field energy matrices (d^7) are solved for different sets of parameters Dq and B. The parameters which give good fit of the calculated and observed band positions are $Dq = 920$ and $B = 820\ cm^{-1}$.

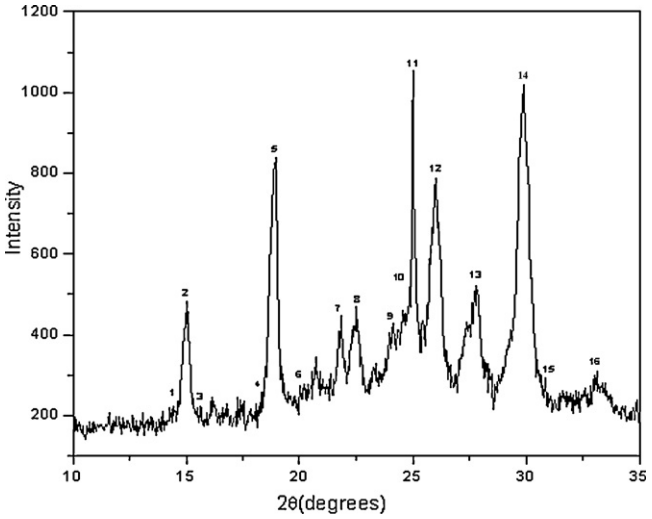

Fig. 4. XRD spectrum of Mn(II) complex.

3.6. Surface morphological studies

X-ray powder diffraction (XRD) of samples are depicted in Figs. 4 and 5, respectively. The observed diffraction data is given in Tables 3 and 4. Using trial and error methods, the unit cell parameters of Mn(II) complex are found to be $a = 11.0469$ Å, $b = 6.2096$ Å, $c = 7.4145$ Å, $\alpha = 90.646^\circ$, $\beta = 95.127^\circ$, $\gamma = 104.776^\circ$ and cell volume $V = 489.7$ Å^3. For Co(II) complex, $a = 9.3236$ Å, $b = 10.2410$ Å, $c = 7.8326$ Å, $\alpha = 90.694^\circ$, $\beta = 99.694^\circ$, $\gamma = 100.476^\circ$ and cell volume $V = 724.2$ Å^3. This data of the complexes support triclinic systems. The observed X-ray pattern of the free ligand sample studied in

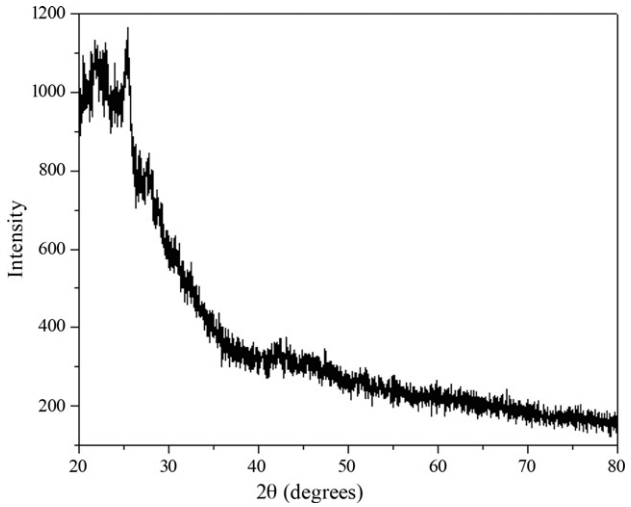

Fig. 3. XRD spectrum of free ligand.

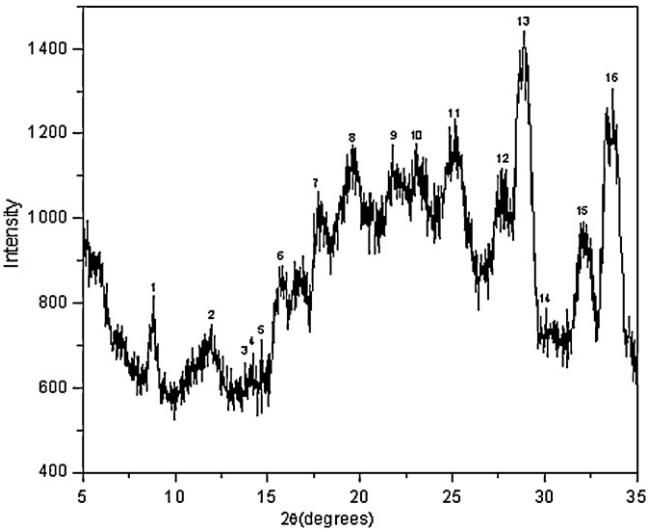

Fig. 5. XRD spectrum of Co(II) complex.

Table 2
Observed and calculated band positions of Co(II) complex.

Transition	Observed band position		Calculated wave numbers (cm^{-1})
	Wave length (nm)	Wave number (cm^{-1})	
$^4T_{1g}(F) \rightarrow {}^4T_{2g}(F)$	1130	8847	8090
$^4T_{1g}(F) \rightarrow {}^4A_{2g}(F)$	600	16,662	17,290
$^4T_{1g}(F) \rightarrow {}^4T_{1g}(P)$	520	19,226	19,280

Table 3
Powder X-ray diffraction data of Mn(II) complex.

Peak number	*d*-spacing (Å)		2θ values		Δ 2θ	(*hkl*)
	Observed	Calculated	Observed	Calculated		
1	6.0038	6.0038	14.74	14.74	0.000	(0 1 0)
2	5.9141	5.9141	14.97	14.97	0.000	($\bar{1}$ 0 1)
3	5.8270	5.8270	15.19	15.19	0.000	(1 0 1)
4	4.7370	4.7370	18.72	18.72	0.000	(1 1 0)
5	4.6859	4.6859	18.92	18.92	0.000	(0 $\bar{1}$ 1)
6	4.6314	4.6314	19.15	19.15	0.000	(0 1 1)
7	4.0795	4.0795	21.79	21.77	0.023	($\bar{1}$ $\bar{1}$ 1)
8	3.9576	3.9008	22.45	22.78	0.331	(1 1 1)
9	3.5779	3.5889	24.86	24.86	−0.078	($\bar{1}$ 0 2)
10	3.5463	3.5463	25.09	25.09	−0.001	(3 0 0)
11	3.4574	3.4648	25.75	25.69	0.056	($\bar{3}$ 1 0)
12	3.3991	3.3953	26.19	26.22	−0.030	(1 0 2)
13	3.1887	3.1867	27.96	27.97	−0.018	($\bar{1}$ 1 2)
14	3.0054	3.0019	29.70	29.74	−0.035	(0 2 0)
15	2.9616	2.9570	30.15	30.20	−0.047	($\bar{2}$ 2 0)
16	2.7121	2.7138	33.00	33.98	0.022	(1 2 0)

Table 4
Powder X-ray diffraction data of Co(II) complex.

Peak number	*d*-spacing (Å)		2θ values		Δ 2θ	(*hkl*)
	Observed	Calculated	Observed	Calculated		
1	10.0605	10.0605	8.78	8.78	0.000	(0 1 0)
2	7.4455	7.4455	11.88	11.88	0.000	($\bar{1}$ 1 0)
3	6.4426	6.4426	13.73	13.73	0.000	($\bar{1}$ 0 1)
4	6.2559	6.2559	14.15	14.15	0.000	(0 $\bar{1}$ 1)
5	5.9949	5.9949	14.76	14.76	0.000	(0 1 1)
6	5.6795	5.6795	15.59	15.59	0.000	($\bar{1}$ 1 1)
7	5.0249	5.0302	17.64	17.62	0.019	(0 2 0)
8	4.5504	4.5146	19.49	19.65	−0.156	(2 0 0)
9	4.0808	4.0825	21.76	21.75	0.009	(1 2 0)
10	3.8638	3.8588	23.00	23.03	−0.030	(2 1 0)
11	3.5502	3.5492	25.06	25.07	−0.007	(0 1 2)
12	3.2149	3.2165	27.73	27.71	0.015	(2 $\bar{2}$ 1)
13	3.1019	3.0994	28.76	28.78	−0.024	($\bar{1}$ 3 1)
14	3.0802	3.0804	28.96	28.96	0.002	($\bar{1}$ 2 2)
15	2.7723	2.7799	32.26	32.17	0.090	($\bar{3}$ 2 1)
16	2.6567	2.6561	33.71	33.71	−0.008	(1 2 2)

the present investigation indicates amorphous nature (Fig. 3). To evaluate the crystallite size of the synthesized complexes, *D* is determined using Debye–Scherer formula [35,36] given by

$$D = \frac{0.94\lambda}{\beta \cos\theta}$$

where β is the full width at half maximum of the predominant peak and θ is the diffraction angle and λ is the wavelength of light. The sizes of the crystallites of the Mn(II) and Co(II) complexes are found to be 50 nm and 55 nm.

Table 5
Antibacterial screening data of the ligand and its Mn(II) and Co(II) complexes (diameter of zone of inhibition in mm).

Compound	*K. pnuemoniae*	*E. coli*	*B. subtilis*	*S. aureus*
Ligand (L)	–	–	–	–
Mn(II) complex	30	21	23	18
Co(II)complex	26	16	20	20
Ampicillin	43	40	43	42
Tetracycline	32	33	30	32

3.7. Antibacterial activity

Antibacterial activity of these metal complexes is tested against different micro-organisms using only one concentration of these metal complexes and their activities are compared with standard antibiotics such as ampicillin and tetracycline (Table 5). The complexes of Mn(II) and Co(II) with free ligand have shown a strong activity against gram-negative bacteria (*E. coli* and *K. pneumoniae*) and gram-positive bacteria (*S. aureus* and *B. subtilis*).

The synthesized ligand and its metal complexes have been screened for reduction in DPPH free radicals and inhibition of iron(III) induced lipid peroxidation at 100 μm concentration. The

Table 6
Effect of ligand and its metal complexes on scavenging of DPPH and Fe^{3+} induced lipid peroxidation at 100 μM concentration.

Compound	DPPH scavenging (%)	Fe^{3+} induced lipid peroxidation
Ligand (L)	42	60
Mn(II) complex	–	–
Co(II) complex	38	41
α-Tocopherol	53	65

free ligand and Co(II) complex show comparable activity in DPPH scavenging and ferric ion induced lipid peroxidation as seen in the case of standard antioxidant α-tocopherol, but Mn(II) complex has not shown any activity (Table 6).

4. Conclusions

In this paper, the ligand benzyloxybenzaldehyde-4-phenyl 3-thiosemcarbazone is synthesized and its structure is investigated. The Mn(II) and Co(II) complexes are prepared with the ligand and they are characterized with analytical and spectral techniques. The EPR and electronic spectral studies of both the complexes indicate near octahedral site symmetry for the metal ions. The ligand does not exhibit any antibacterial activity but both the complexes give considerable antibacterial activity. Free ligand and the Co(II) complex give good activity in DPPH scavenging and ferric ion induced lipid peroxidation but the Mn(II) complex does not exhibit these activities.

Acknowledgements

Two of the authors B. Prathima and Y. Subba Rao are highly grateful to the UGC, Government of India, and New Delhi for financial assistance in the form of an award of Meritorious Research Fellowship. We sincerely thank Prof. J. Lakshmana Rao, Department of Physics, S. V. University, Tirupati, for his help in EPR studies. We also thank K. Madhavi, Institute of Pharmaceutical Technology, Sri Padhmavati Mahila VisvaVidyalayam, Tirupati, for her help in biological studies.

References

[1] N.K. Singh, A. Srivastava, Trans. Met. Chem. 25 (2000) 133.
[2] S. Chandra, A. kumar, Spectrochim. Acta Part A 67 (2007) 697.
[3] S. Chandra, L.K. Gupta, K.K. Sharma, J. Saudi Chem. Soc. 9 (2005) 131.
[4] E.M. Jouad, G. Larcher, M. Allain, J. Inorg. Biochem. 86 (2001) 565.
[5] P. Tarasconi, S. Capacchi, G. Pelosi, M. Cornia, R. Albertini, A. Bonati, P.P. Dall, P. Luunghi, S. Pinelli, Bioorg. Med. Chem. 8 (2000) 157.
[6] D. María, C. Rodríguez-Argüelles, P. Tourón-Touceda, Roberto Cao, Ana. M. García-Deibe Paolo Pelagatti, Corrado Pelizzi, Franca Zani, J. Inorg. Biochem. 103 (2009) 35.
[7] S. Chandra, X. Sangeetika, Spectrochim. Acta Part A 60 (2004) 147.
[8] M. Wang, L.F. Wang, Y.Z. Ligands, Q.X. Li, Trans. Met. Chem. 26 (2001) 307.
[9] I. Ana, Matesanz, Pilar Souza, J. Inorg. Biochem. 101 (2007) 1354.
[10] D. Kovala-Demertzi, M.A. Demertzis, J.R. Miller, C. Padadopoulou, C. Dodorou, G. Filousis, J. Inorg. Biochem. 86 (2001) 555.
[11] A.G. Quiroga, J.M. Peĭrez, L. Solera, J.R. Masaguer, A. Luque, P. Roman, A. Edwards, C. Alonso, C.N. Ranninger, J. Med. Chem. 41 (1998) 1399.
[12] D. Kovala-Demertzi, A. Domopoulou, M.A. Demertzis, G. Valle, A. Papageorgiou, J. Inorg. Biochem. 68 (1997) 147.
[13] D.T. Minkel, D.H. Petering, Cancer Res. 38 (1978) 117.
[14] K. Uesugi, L.J. Sik, H. Nishioka, T. Kumagai, T. Nagahiro, J. Microchem. 50 (1994) 88.
[15] M.Y. Khuhawar, G.M. Arain, Talanta 68 (2006) 535.
[16] P. Novak, K. Pic˘uljan, T. Biljan, T. Hrenar, Z. Meicˇ, J. Mol. Struct. 919 (2009) 66.
[17] B. Prathima, Y. Subba Rao, S. Adinarayana Reddy, Y.P. Reddy, A. Varada Reddy, Spectrochim. Acta Part A 71 (2010) 248.
[18] A.W. Bauer, W.M. Kirby, J.C. Sherris, M. Turck, Am. J. Clin. Pathol. 45 (1966) 493.
[19] C. Sheikh, M.S. Hossain, M.S. Easmin, M.S. Islam, M. Rashid, Biol. Pharm. Bull. 27 (2004) 710.
[20] M.S. Baliga, G.C. Jagetia, P. Venkatesh, R. Reddy, J.N. Ulloor, Br. J. Radiol. 77 (2004) 1027.
[21] K. Bharathi, G. Swarnalatha, S.K.A. Begum, K. Prasad, J. Pharm. Res. 7 (2008) 78.
[22] S. Jayan, M.N.A. Rao, J. Pharm. Pharmacol. 46 (1994) 1013.
[23] J.M. Braughler, L.A. Duncan, R.L. Chase, J. Biol. Chem. 261 (1986) 10282.
[24] R.V.S.S.N. Ravikumar, K. Ikeda, A.V. Chandrasekhar, Y.P. Reddy, P.S. Rao, J. Yamauchi, J. Phys. Chem. Solids 64 (2003) 2433.
[25] A.V. Chandrasekhar, R.V.S.S.N. Ravi Kumar, B.J. Reddy, Y.P. Reddy, P.S. Rao, Phys. Chem. Glasses 43 (2002) 173.
[26] D. Viviani, F. Faivre, C. Levelut, M. Smaihi, J. Phy. Chem. B 110 (2006) 7281.
[27] L.D. Bogomolova, E.G. Grechko, N.A. Krasil'nikova, V.V. Sakhrov, J. Non-Cryst. Solids 69 (1985) 299.
[28] A. Abragam, B. Bleaney, Electron Paramagnetic Resonance of Transition Ions, Clarendon, Oxford, 1970.
[29] D.L. Griscom, J. Non-Cryst. Solids 40 (1980) 211.
[30] I. Ardelean, M. Peteanu, V. Simon, S. Simon, M. Flora, Phys. Chem. Glasses 41 (2000) 153.
[31] Y. Tanabe, S. Sugano, J. Phys. Soc. Jpn. 9 (1954) 753.
[32] S. Chandra, A. Gautam, J. Saudi Chem. Soc. 74 (2009) 1413.
[33] S. Chandra, A. kumar, Spectrochim. Acta Part A 68 (2007) 469.
[34] A.B.P. Lever, Inorganic Electronic Spectroscopy, second ed., Elsevier Publishing Co., Amsterdam, 1984.
[35] M.R. Prathapchandra Kurup, P.E. Rapheal, E. Mano, E. Suresh, Polyhedron 26 (2007) 607.
[36] B.E. Warren, X-ray Diffraction, Dover, New York, 1990, p. 253.